STRUCTURAL BIOLOGY COMMUNICATIONS

ISSN 2053-230X

Expression, crystallization and preliminary crystallographic data analysis of VioD, a hydroxylase in the violacein-biosynthesis pathway

Tingting Ran,[a] Mengxiao Gao,[a] Qiaoe Wei,[a] Jianhua He,[b] Lin Tang,[b] Weiwu Wang[a] and Dongqing Xu[a]*

[a]Department of Microbiology, Nanjing Agricultural University, Nanjing, People's Republic of China, and [b]Shanghai Institute of Applied Physics, Chinese Academy of Sciences, Shanghai, People's Republic of China. *Correspondence e-mail: dqxu@njau.edu.cn

Received 25 November 2014
Accepted 18 December 2014

Keywords: violacein; VioD.

Supporting information: this article has supporting information at journals.iucr.org/f

Violacein, a natural purple secondary metabolite, is sequentially biosynthesized by five enzymes in the following pathway: VioA–VioB–VioE–VioD–VioC. VioD, a flavin-dependent oxygenase, catalyzes the hydroxylation of the intermediate product prodeoxyviolaceinic acid (PVA) at the 5-position of one indole ring to yield proviolacein. *In vitro* biochemical data have revealed this process, but the catalytic mechanism still remains largely unclear. Here, the cloning, expression, purification, crystallization and diffraction of VioD are reported. Crystals of VioD diffracted to 1.7 Å resolution and belonged to space group $P3_1$, with unit-cell parameters $a = b = 90.0$, $c = 94.5$ Å, $\alpha = \beta = 90$, $\gamma = 120^\circ$. Solvent-content calculation and molecular-replacement results suggest the presence of two molecules of VioD in the asymmetric unit.

1. Introduction

Violacein {3-[1,2-dihydro-5-(5-hydroxy-1*H*-indol-3-yl)-2-oxo-3*H*-pyrrol-3-ylidene]-1,3-dihydro-2*H*-indol-2-one}, a natural purple secondary metabolite, is produced by several Gram-negative bacteria such as *Chromobacterium violaceum* (Durán & Menck, 2001; Dessaux *et al.*, 2004; Hoshino, 2011), *Janthinobacterium lividum* (Pantanella *et al.*, 2007; Schloss *et al.*, 2010), *Pseudoalteromonas tunicata* (Egan *et al.*, 2002), some *Duganella* sp. strains (Jiang *et al.*, 2010; Aranda *et al.*, 2011) and some other bacteria. Violacein has attracted significant interest for potential pharmacological applications owing to its various nonphysiological functions, including broad-spectrum antibacterial activity, especially against Gram-positive bacteria (Durán *et al.*, 1994; Durán & Menck, 2001), antiviral (Andrighetti-Fröhner *et al.*, 2003), trypanocidal (Riveros *et al.*, 1988), antiprotozoan (Matz *et al.*, 2004), antioxidant (Konzen *et al.*, 2006), anti-ulcerogenic (Durán *et al.*, 2003) and anti-tumour activities (Bromberg *et al.*, 2010; Martins *et al.*, 2010).

The gene clusters for violacein biosynthesis from different bacteria have been identified and sequenced; they all consist of five genes, *vioA–vioE*, encoding five enzymes (Pemberton *et al.*, 1991; August *et al.*, 2000; Brady *et al.*, 2001). The five enzymes catalyze the formation of violacein sequentially in the following pathway: VioA–VioB–VioE–VioD–VioC (Momen & Hoshino, 2000; Balibar & Walsh, 2006). VioA, a flavin-dependent tryptophan 2-monooxygenase, catalyzes the oxidization of tryptophan to form indole-3-pyruvic acid imine (IPA). IPA is then dimerized by VioB to produce a short-lived compound X (IPA imine dimer). In the presence of VioE, compound X is enzymatically transformed into prodeoxyviolaceinic acid (PVA). The last two enzymes, VioC and VioD,

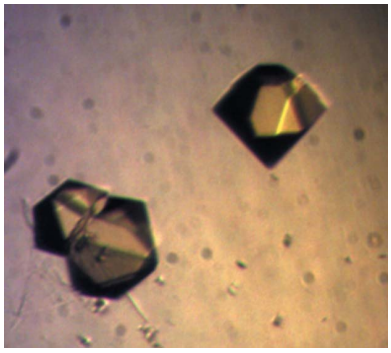

Table 1
Macromolecule-production information.

Source organism	*Duganella* sp. ZLP-XI
DNA source	Chromosomal DNA of *Duganella* sp. ZLP-XI
Forward primer†	CGGTAGCTAGCATGAAGATTCTCGTGATCGGCG
Reverse primer‡	TACCTCGAGACGGCCCAGGGCGTAGCCCAG
Cloning vector	pET-28a
Expression vector	pET-28a
Expression host	*E. coli*
Complete amino-acid sequence of the construct produced	MGSSHHHHHHSSGLVPRGSHMASMKILVIGAG-PAGLIFASQMKQAQPGWDISIVEKNTQEEV-LGWGVVLPGRPPRHPANPLSYLEQPERLNP-QYLEEFKLVHHDQPNLMSTGVTLCGVERRG-LVQALRAKCVAAGIAISYETPPASQAQLEA-EYDLVVVANGVNHKTLQLPPSLAPQIDFGR-NKYIWYGTTQLFDQMNLVFRSNAQGMFIGH-AYRYSDTMSTFVVECDEQAYARAELEMRSE-RDAAAYIAKVFEAELGGHALVSQPGQGWRN-FMTLSRERACEGKFVLIGDALQSGHFSIGH-GTTMAVVLALLLVKTLSADTDPVAALDNFN-ARALPLAHLFRDHANSSRLWFESVAERMEL-SNADLTASFDARRKDLPPLQDALMASLGYA-LGRLEHHHHHH

† The NheI site is underlined. ‡ The XhoI site is underlined.

are both flavin-dependent oxygenases. VioD hydroxylates PVA at the 5-position of one indole ring to yield proviolacein; VioC then oxidizes at the 2-position of the other indole ring to generate the oxindole to yield the end product violacein (Balibar & Walsh, 2006; Sanchez *et al.*, 2006; Asamizu *et al.*, 2007; Shinoda *et al.*, 2007). Although some biochemical data on the mechanism of violacein biosynthesis have been reported, little is known about the structures of the five enzymes involved in the synthetic pathway of violacein, with the exception of VioE. The VioE structure is a homodimer and each monomer adopts a conformation that resembles an opened baseball glove (Hirano *et al.*, 2008). To elucidate the mechanism of VioD, we cloned and expressed the gene for VioD in *Escherichia coli*; the recombinant VioD was then purified and crystallized.

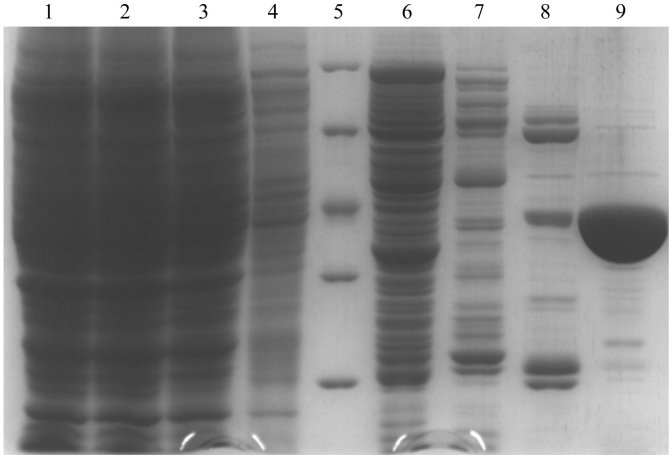

Figure 1
Coomassie-stained SDS–PAGE analysis of VioD purified by IMAC. The contents of the lanes are as follows: lane 1, whole cell lysate; lane 2, supernatant of centrifugation after sonication; lane 3, flowthrough after the supernatant was loaded onto an Ni–NTA column; lane 4, protein sample washed with binding buffer containing 5 m*M* imidazole; lane 5, molecular-weight marker; lanes 6 and 7, protein samples washed with binding buffer containing 20 and 50 m*M* imidazole, respectively; lanes 8 and 9, target protein eluted with buffer containing 100 and 250 m*M* imidazole, respectively. The molecular weights of the markers from the top to the bottom are 116.0, 66.2, 45.0, 35.0 and 25.0 kDa, respectively, and that of the heterogeneously expressed VioD protein is 43 kDa.

2. Materials and methods

2.1. Macromolecule production

The *vioD* gene (GenBank KJ131413) was amplified by PCR using the chromosomal DNA of the violacein-producing strain *Duganella* sp. ZLP-XI as the template. The forward and the reverse primers (Table 1) contained NheI and XhoI restriction sites, respectively. The PCR product was purified and digested by NheI and XhoI and then ligated into pET-28a vector, which was digested by the same restriction enzymes to generate the expression plasmid pET-28a-VioD. The recombinant plasmid was verified by DNA sequencing and transformed into *E. coli* C43 (DE3) cells. The final sequence of the protein is shown in Table 1.

Cells harbouring the pET-28a-VioD plasmid were grown at 310 K until the OD_{600} reached about 1.0; isopropyl β-D-1-thiogalactopyranoside (IPTG) was then added to the medium to a final concentration of 0.5 m*M* and the culture was grown for a further 3 h at 303 K for protein expression. The cells were harvested by centrifugation at 5000 rev min^{-1} at 277 K for 5 min. The cell pellet was resuspended in binding buffer (50 m*M* KH_2PO_4/K_2HPO_4 pH 7.6, 300 m*M* NaCl, 5 m*M* imidazole, 10% glycerol). The cells were then lysed by sonication on ice for 30 min at an output of 200 W and clarified by centrifugation at 12 000 rev min^{-1} for 30 min at 277 K. The supernatant was loaded onto an Ni–NTA column (GE Healthcare Life Science, Uppsala, Sweden) pre-equilibrated with binding buffer and then washed with binding buffer containing 10, 20 and 50 m*M* imidazole (six column volumes each); the recombinant protein was then eluted with elution buffers containing 100 and 250 m*M* imidazole (six column volumes each). The purity and molecular mass of the

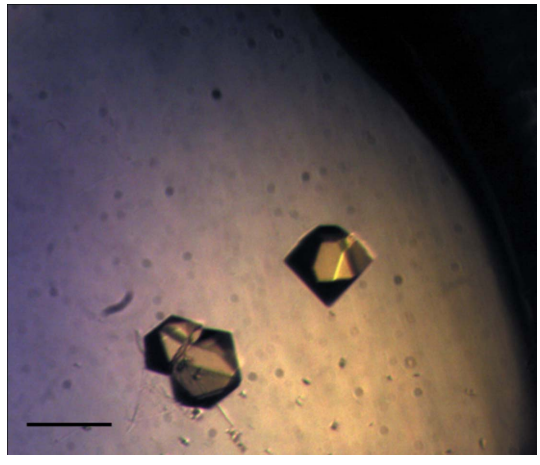

Figure 2
Crystals of VioD. The crystals shown are about 0.1 × 0.1 × 0.1 mm in size. The scale bar is 100 µm in length.

Table 2
Crystallization.

Method	Sitting-drop vapour diffusion
Plate type	48-well
Temperature (K)	295
Protein concentration (mg ml^{-1})	15 and 7.5
Buffer composition of protein solution	20 m*M* Tris–HCl pH 8.0, 300 m*M* NaCl, 10% glycerol
Composition of reservoir solution	3.5 *M* sodium formate pH 7.0
Volume and ratio of drop	1 µl protein and 1 µl reservoir
Volume of reservoir (µl)	50

recombinant protein were analyzed using 12%(*w*/*v*) SDS–PAGE (Laemmli, 1970; Fig. 1). The fractions containing VioD were collected and concentrated using 30 kDa molecular-weight cutoff Amicon Ultra centrifugal filters (Millipore). The concentrated protein was then loaded onto a manually packed 30 ml Superdex 200 column (GE Healthcare Life Science, Uppsala, Sweden) which was pre-equilibrated with 20 m*M* Tris–HCl pH 8.0, 300 m*M* NaCl, 10% glycerol. The protein was eluted with the same buffer and the elution pattern showed only one peak. The peak fraction containing VioD was pooled and the purity of the VioD was analyzed by SDS–PAGE (Supplementary Fig. S1). All protein-purification steps were performed at 277 K.

2.2. Crystallization

Purified VioD was concentrated to 15 mg ml^{-1} as calculated by assuming an absorbance of 0.99 at 280 nm for a 1.0 mg ml^{-1} protein solution based on an ε_{280} of 44 140 M^{-1} cm^{-1}. The crystallization experiments were performed manually using the sitting-drop vapour-diffusion technique at 295 K in 48-well plates. Commercial screens from Hampton Research (Crystal Screen, Crystal Screen 2, MembFac, Crystal Screen Cryo, Crystal Screen Lite, PEGRx 1, PEGRx 2 and Index) and Microlytic (MCSG1–4) were used for crystallization trials with protein concentrations of 15 and 7.5 mg ml^{-1}. In the crystallization setup, 1 µl VioD solution was mixed with 1 µl reservoir solution and the droplet was equilibrated against 50 µl reservoir solution. The initial crystallization screen yielded diamond-like crystals from condition No. 25 of Index (3.5 *M* sodium formate pH 7.0; Fig. 2, Table 2) and rod-shaped crystals from condition No. 6 of MCSG1 (0.2 *M* ammonium sulfate, 0.1 *M* bis-tris–HCl pH 5.5, 25% PEG 3350). The crystals obtained from condition No. 25 of Index diffracted better than the crystals obtained from the other condition. Diamond-like crystals (Fig. 2) grew to full size with dimensions of approximately 0.1 × 0.1 × 0.1 mm in two weeks.

2.3. Data collection and processing

Before data collection, the VioD crystals were quickly immersed in reservoir solution supplemented with 15%(*v*/*v*) glycerol as a cryoprotectant for a few seconds and were then mounted on nylon loops. The mounted crystals were flash-cooled by plunging them quickly into liquid nitrogen. Complete X-ray diffraction data sets were collected on beamline BL17U1 at SSRF at a wavelength of 0.9791 Å using an ADSC Quantum 315r CCD area detector. The diffraction frames were collected with a 1° oscillation range and 0.4 s per frame with a 250 mm distance between the crystal and the detector. The diffraction data were indexed and integrated using the *XDS* package (Kabsch, 2010*a*,*b*) and were scaled with *SCALA* (Evans, 2006). Molecular replacement was attempted using the structure of a VioD homologue from *C. violaceum* (PDB entry 3c4a; Northeast Structural Genomics Consortium, unpublished work) as a template with the *BALBES* pipeline (Long *et al.*, 2008). Data-collection and processing statistics are summarized in Table 3.

Table 3
Data collection and processing.

Values in parentheses are for the outer shell. Because $I/\sigma(I)$ in the 1.9–1.8 Å resolution shell was 3.33 and the *R* factor for the 1.8–1.7 Å resolution shell was not high, we chose to keep the data to 1.7 Å resolution.

Diffraction source	BL17U, SSRF
Wavelength (Å)	0.9791
Temperature (K)	100
Detector	ADSC Quantum 315r CCD
Crystal-to-detector distance (mm)	250
Rotation range per image (°)	1
Total rotation range (°)	180
Exposure time per image (s)	0.4
Space group	$P3_1$
Unit-cell parameters (Å, °)	$a = b = 90.0$, $c = 94.5$, $\alpha = \gamma = 90$, $\beta = 120$
Mosaicity (°)	0.104
Resolution range (Å)	20–1.7 (1.80–1.70)
Total No. of reflections	522557 (65031)
No. of unique reflections	93564 (14152)
Completeness (%)	99.2 (95.4)
$\langle I/\sigma(I)\rangle$	9.8 (1.74)
Multiplicity	5.59 (4.60)
$R_{\rm r.i.m.}$ (%)	11.4 (93.6)
Overall *B* factor from Wilson plot (Å^2)	32.279

3. Results and discussion

Recombinant VioD protein was solubly overexpressed in *E. coli*. The recombinant VioD was purified in a two-step procedure, applying immobilized metal-affinity chromatography (IMAC) and size-exclusion chromatography (SEC), to give a final yield of 15 mg per litre of culture medium. The purity of the purified VioD was greater than 95% and there was only a single band on SDS–PAGE, with an apparent molecular mass of around 43 kDa consistent with the predicted size. Crystals were obtained (Fig. 2) in two different conditions (condition No. 25 from Index and condition No. 6 from MCSG1) and the best crystals suitable for data collection were produced in 3.5 *M* sodium formate pH 7.0. The diamond-like crystals grew to maximum dimensions of 0.1 × 0.1 × 0.1 mm in two weeks and one of them diffracted to 1.7 Å resolution at the synchrotron source (Supplementary Fig. S2). A complete 1.7 Å resolution diffraction data set was collected from a single crystal; the data-collection and processing statistics are given in Table 3. The crystals belonged to space group $P3_1$, with unit-cell parameters $a = 90.0$, $b = 90.0$, $c = 94.5$ Å, $\alpha = \beta = 90$, $\gamma = 120°$. A Matthews coefficient value of 2.51 Å^3 Da^{-1} (Matthews, 1968), which corresponds to a

solvent content of 50.05%, suggests the presence of two VioD molecules in the asymmetric unit of the hexagonal cell.

Molecular replacement was attempted using the structure of a VioD homologue (PDB entry 3c4a) as the search template (67% sequence identity). The result shows two molecules in the asymmetric unit. Manual model building and structure refinement are under way. To elucidate the catalytic mechanism of VioD, crystals of the protein–ligand complex are in preparation.

Acknowledgements

We thank the staff of beamline BL17U1 at SSRF, Shanghai, People's Republic of China for their assistance during data collection. This work was supported by grants from the National Natural Science Foundation of China (31100028 and 31400055), the Natural Science Foundation of Jiangsu Province (BK20140690) and the Youth Science and Technology Innovation Fund from Nanjing Agricultural University (KJ2013027).

References

Andrighetti-Fröhner, C. R., Antonio, R. V., Creczynski-Pasa, T. B., Barardi, C. R. & Simões, C. M. (2003). *Mem. Inst. Oswaldo Cruz*, **98**, 843–848.

Aranda, S., Montes-Borrego, M. & Landa, B. B. (2011). *Microb. Ecol.* **62**, 446–459.

Asamizu, S., Kato, Y., Igarashi, Y. & Onaka, H. (2007). *Tetrahedron Lett.* **48**, 2923–2926.

August, P. R., Grossman, T. H., Minor, C., Draper, M. P., MacNeil, I. A., Pemberton, J. M., Call, K. M., Holt, D. & Osburne, M. S. (2000). *J. Mol. Microbiol. Biotechnol.* **2**, 513–519.

Balibar, C. J. & Walsh, C. T. (2006). *Biochemistry*, **45**, 15444–15457.

Brady, S. F., Chao, C. J., Handelsman, J. & Clardy, J. (2001). *Org. Lett.* **3**, 1981–1984.

Bromberg, N., Dreyfuss, J. L., Regatieri, C. V., Palladino, M. V., Durán, N., Nader, H. B., Haun, M. & Justo, G. Z. (2010). *Chem. Biol. Interact.* **186**, 43–52.

Dessaux, Y., Elmerich, C. & Faure, D. (2004). *Rev. Med. Interne*, **25**, 659–662.

Durán, N., Justo, G. Z., Melo, P. S., De Azevedo, M. B. M., Souza Brito, A. R. M., Almeida, A. B. A. & Haun, M. (2003). *Can. J. Physiol. Pharmacol.* **81**, 387–396.

Durán, N. & Menck, C. F. (2001). *Crit. Rev. Microbiol.* **27**, 201–222.

Durán, N., Antonio, R. V., Haun, M. & Pilli, R. A. (1994). *World J. Microbiol. Biotechnol.* **10**, 686–690.

Egan, S., James, S., Holmström, C. & Kjelleberg, S. (2002). *Environ. Microbiol.* **4**, 433–442.

Evans, P. (2006). *Acta Cryst.* D**62**, 72–82.

Hirano, S., Asamizu, S., Onaka, H., Shiro, Y. & Nagano, S. (2008). *J. Biol. Chem.* **283**, 6459–6466.

Hoshino, T. (2011). *Appl. Microbiol. Biotechnol.* **91**, 1463–1475.

Jiang, P.-X., Wang, H.-S., Zhang, C., Lou, K. & Xing, X.-H. (2010). *Appl. Microbiol. Biotechnol.* **86**, 1077–1088.

Kabsch, W. (2010*a*). *Acta Cryst.* D**66**, 125–132.

Kabsch, W. (2010*b*). *Acta Cryst.* D**66**, 133–144.

Konzen, M., De Marco, D., Cordova, C. A. S., Vieira, T. O., Antônio, R. V. & Creczynski-Pasa, T. B. (2006). *Bioorg. Med. Chem.* **14**, 8307–8313.

Laemmli, U. K. (1970). *Nature (London)*, **227**, 680–685.

Long, F., Vagin, A. A., Young, P. & Murshudov, G. N. (2008). *Acta Cryst.* D**64**, 125–132.

Martins, D., Frungillo, L., Anazzetti, M. C., Melo, P. S. & Durán, N. (2010). *Int. J. Nanomedicine*, **5**, 77–85.

Matthews, B. W. (1968). *J. Mol. Biol.* **33**, 491–497.

Matz, C., Deines, P., Boenigk, J., Arndt, H., Eberl, L., Kjelleberg, S. & Jürgens, K. (2004). *Appl. Environ. Microbiol.* **70**, 1593–1599.

Momen, A. Z. & Hoshino, T. (2000). *Biosci. Biotechnol. Biochem.* **64**, 539–549.

Pantanella, F., Berlutti, F., Passariello, C., Sarli, S., Morea, C. & Schippa, S. (2007). *J. Appl. Microbiol.* **102**, 992–999.

Pemberton, J. M., Vincent, K. M. & Penfold, R. J. (1991). *Curr. Microbiol.* **22**, 355–358.

Riveros, R., Haun, M., Campos, V. & Durán, N. (1988). *Arq. Biol. Tecnol.* **31**, 475–487.

Sanchez, C., Braña, A. F., Méndez, C. & Salas, J. A. (2006). *Chembiochem*, **7**, 1231–1240.

Schloss, P. D., Allen, H. K., Klimowicz, A. K., Mlot, C., Gross, J. A., Savengsuksa, S., McEllin, J., Clardy, J., Ruess, R. W. & Handelsman, J. (2010). *DNA Cell Biol.* **29**, 533–541.

Shinoda, K., Hasegawa, T., Sato, H., Shinozaki, M., Kuramoto, H., Takamiya, Y., Sato, T., Nikaidou, N., Watanabe, T. & Hoshino, T. (2007). *Chem. Commun.*, pp. 4140–1412.